Morphology and Histochemistry of Infralabial Glands of Two Species in the Slug-Eating Family Pareidae (Reptilia: Serpentes)

Dan WANG[1,2], Jinlong REN[1,2], Ke JIANG[1], Wei WU[1,2], Changjun PENG[1,2], Hussam ZAHER[3], Dechun JIANG[1*] and Jiatang LI[1,2,4*]

[1] CAS Key Laboratory of Mountain Ecological Restoration and Bioresource Utilization, Ecological Restoration and Biodiversity Conservation Key Laboratory of Sichuan Province, Chengdu Institute of Biology, Chinese Academy of Sciences, Chengdu 610041, Sichuan, China

[2] University of Chinese Academy of Sciences, Beijing 100049, China

[3] Museu de Zoologia, Universidade de São Paulo, São Paulo 04263-000, SP, Brazil

[4] Southeast Asia Biodiversity Research Institute, Chinese Academy of Sciences, Yezin Nay Pyi Taw 05282, Myanmar

Abstract Pareidae and Dipsadidae, two independently evolved taxa in the Serpentes lineage, both feed exclusively on terrestrial mollusks (snails and slugs). Dipsadid snakes developed hypertrophic infralabial glands in their lower jaw, which are thought to be associated with their specialized feeding behaviors. However, whether a similar gland exists in pareid snakes is unknown. In this study, we examined the morphological characteristics of the infralabial glands in *Pareas berdmorei* and *Pareas chinensis* based on comparative anatomical, histochemical, and histopathological analysis. Our results demonstrated that both *Pareas* species had similar hypertrophied infralabial glands in the lower jaw, which consisted of tubules with mucinous properties and seromucous acini. The secretory granules of the seromucous cells also showed high electron density. The cytoplasm was rich in rough endoplasmic reticulum, mitochondria, and Golgi apparatus, suggesting that these cells may secrete protein substances, and play an important role in digesting mollusks. This study provides evidence of morphological convergence between Pareidae and Dipsadidae due to specialized diet adaptation, which will be the foundation for prospective functional research.

1. Introduction

Snakes display exceptionally diversified feeding habits. Some groups consume a wide variety of animals including both vertebrates and invertebrates, while others exhibit strong dietary specialization (Greene, 1997; Lillywhite, 2014; Zug, 1993) such as crustacean-eating snakes, egg-eating snakes, and ant/termite-eating blind snakes (Scolecophidia) (Broadley, 1979; Coleman *et al.*, 1993; Jayne *et al.*, 2018; Webb *et al.*, 2000). Many snakes within the family Dipsadidae are considered specialists, feeding solely on terrestrial mollusks, e.g., snails of the genus *Drymaeus* and slugs of the genus *Sarasinula* (Cundall and Greene, 2000; Dunn, 1951; Peters, 1960; Sazima, 1989). Some genera within Dipsadidae have developed hypertrophied and specialized infralabial glands in their lower jaw. These glands produce secretory products that are predominantly serous in nature and may be related to the specialized mollusk diet (de Oliveira *et al.*, 2014; de Oliveira *et al.*, 2008; Zaher *et al.*, 2014). Notably, injection of infralabial gland extracts in the visceral mass of snails can result in paralysis and, in some cases, death (Laporta-Ferreira and Salomão, 1991; Salomão and Laporta-Ferreira, 1994). For example, the infralabial glands of the neotropical slug-eating snake *Sibynomorphus mikani* contain a high protein content, and extract-injected slugs show an increase in mucus secretion, contortions, and immobilization of the body (Salomão and Laporta-Ferreira, 1994). Thus, infralabial gland specialization in some genera of Dipsadidae may be useful for neutralization of mollusk secretions and later digestion.

---

* Corresponding authors: Dr. Jiatang LI, from Herpetological Museum, Chengdu Institute of Biology (CIB), Chinese Academy of Sciences (CAS), Chengdu, Sichuan, China, with his research focusing on taxonomy, phylogenetics, biogeography, genomics and evolution of amphibians and reptiles; Dr. Dechun JIANG, from CIB, CAS, Chengdu, Sichuan, China, with her research focusing on phylogenetics, biogeography, and evolution of amphibians and reptiles.
E-mail: lijt@cib.ac.cn (Jiatang LI); jiangdc@cib.ac.cn (Dechun JIANG)

Snakes in the Southeast Asian family Pareidae are also considered dietary specialists, preying exclusively on terrestrial snails and slugs (Cundall and Greene, 2000). The family Pareidae, which is widely distributed across South and Southeast Asia, currently consists of four genera: i.e., *Pareas* Wagler, 1830; *Aplopeltura* Duméril, 1853; *Asthenodipsas* Peters, 1864; and *Xylophis* Beddome, 1878 (Deepak *et al.*, 2018; Wang *et al.*, 2020; Zhao, 2006; Poyarkov *et al.*, 2022). These snakes exhibit several morphological changes associated with specialized foraging behavior, such as asymmetry in the number of mandibular teeth (Hoso *et al.*, 2007). Almost all pareid snakes, except for non-snail-eating specialists, have more teeth in the right mandible than the left for functional specialization in feeding on the dextral majority of land snails (Hoso, 2017). Fewer teeth in the left mandible may be useful for smoothly biting the sticky tissue of snails, while more teeth in the right mandible may be useful for firmly grasping (Chang *et al.*, 2021; Hoso, 2017; Hoso *et al.*, 2007). Specialization of skull morphology is also found in some pareid and dipsadid snakes, including short snout and pterygoids, reduced supratemporals, long mandibles, and complete separation of the posterior end of the pterygoid from the quadrato-mandibular joint. This connection makes the mandible more flexible, which can help when preying on terrestrial snails (dos Santos *et al.*, 2017; Kojima *et al.*, 2020). Although specialized feeding behavior and associated morphological changes are well documented in the family Pareidae (Danaisawadi *et al.*, 2016; Götz, 2002), it remains unknown whether well-developed infralabial glands similar to those found in dipsadid snakes also exist in this Asian slug-eating group.

In the current study, we investigated infralabial glands and associated structures in pareid snakes and correlated gland structure with secretion biochemistry and the peculiar feeding habits of this group. We focused on morphology, histochemistry, and arrangement of different cell types within the secretory units of the infralabial glands of two species of *Pareas*. This work will provide a foundation for further research on the functional mechanisms of these specialized glands.

2. Materials and Methods

2.1. Samples collection and processing Three individuals of *P. berdmorei* were collected from Mengla county, Xishuangbanna, Yunnan Province, China and three individuals of *P. chinensis* were from Mt. Emei, Leshan city, Sichuan Province, China in this work. An adult male of *P. berdmorei* (total length 620 mm) was used to predation experiment. The snake was starved for three days before the predation experiment, and the snake was then placed on a dissecting tray with dead leaves (41.5 cm length

× 31.2 cm width × 3.5 cm height), three snails of equal size were placed in front of the snake. At a distance of one meter from the snake, we used the camera equipped in the laboratory to film the whole process of preying on the snail. On the basis of existing specimens in the laboratory, we selected snakes with different feeding habits. A total of other four families, including nine genera and 16 species were used for comparison of infralabial gland (Table 1). The specimens were euthanized via an intraperitoneal injection of sodium thiopental, and then we removed the entire head from the specimens at the first cervical vertebra and skinned off the head. The infralabial glands were dissected individually for histological and histochemistry study. All specimens in this work were preserved in the Herpetological Museum, Chengdu Institute of Biology (CIB), Chinese Academy of Sciences (CAS), Chengdu, Sichuan, China.

The entire head was fixed in 10% neutral formalin fixative solution for 24 h and subsequently submitted to decalcification in 4.13% aqueous EDTA, pH 7.2, renewed every other three days, and kept in constant stirring for a month. After head decalcification was completed, the entire head was divided into left and right parts from the middle, put the head in gradient ethanol for dehydration, and embedded in paraffin, and submitted to serial sagittal or transversal sectioning. We used pathology slicer of Shanghai Leica Instruments Co., Ltd, model RM2016 to obtain sections of 4 μm. Dissected infralabial glands were fixed in 4% paraformaldehyde with PBS 0.1 M, pH 7.2 for 24 h, and in gradient ethanol for dehydration, and embedded in paraffin, and conducted to serial sagittal or longitudinal sectioning. We used same pathology slicer to obtain glandular sections of 4 μm.

2.2. Histology and histochemistry All sections of the head were stained with hematoxylin-eosin (HE) staining for general study of the tissues. A group of three sections of infralabial glands were stained with hematoxylin-eosin (HE) staining for general study of the tissues. The remaining four groups glandular sections were used to following histochemical staining steps, the alcian blue (AB) pH 2.5, periodic acid-Schiff (PAS) and combined alcian blue (AB) pH 2.5 and periodic acid-Schiff (PAS) for identification of acid and natural mucosubstances, and Coomassie brilliant blue R250 for identification of protein (Kiernan, 2015).

2.3. Transmission electron microscopy Fresh tissues were selected to minimize mechanical damage such as pulling, contusion and extrusion. We used a sharp blade to quickly cut and harvest fresh tissue blocks within 1–3 min. The size of tissue block should be no more than 1 mm³. The removed tissue block was immediately put into 2.5% glutaraldehyde fixative solution for 24 h (Sabatini *et al.*, 1963), which was fixed at 4 ℃ for preservation and transportation. Tissues were fixed in 1%

Table 1 Information on voucher numbers and localities of 16 snake species used in this study.

Family	Species	Voucher No.	Localities
Pareidae	*Pareas berdmorei*	CIB 119346	Jinghong, Yunnan, China
Pareidae	*Pareas chinensis*	CIB 119351	Wenxian, Gansu, China
Pareidae	*Pareas formosensis*	CIB 119336	Leishan, Guizhou, China
Pareidae	*Pareas nigriceps*	CIB 119350	Anlong, Guizhou, China
Colubridae	*Lycodon rufozonatus*	CIB 119349	Anlong, Guizhou, China
Colubridae	*Boiga multomaculata*	CIB 119344	Shenlongjia, Hubei, China
Colubridae	*Oreocryptophis porphyraceus*	CIB 119342	Leishan, Guizhou, China
Colubridae	*Pseudoxenodon macrop*	CIB 119337	Leishan, Guizhou, China
Colubridae	*Boiga multomacula*	CIB 119347	Jinghong, Yunnan, China
Colubridae	*Boiga cyanea*	CIB 119340	Jinghong, Yunnan, China
Colubridae	*Ahaetulla prasina*	CIB 119339	Jinghong, Yunnan, China
Viperidae	*Trimeresurus guoi*	CIB 119348	Jinghong, Yunnan, China
Viperidae	*Protobothrops mucrosquamatus*	CIB 119341	Pengzhou, Sichuan, China
Viperidae	*Protobothrops jerdonii*	CIB 119343	Mianning, Sichuan, China
Elapidae	*Bungarus multicinctus*	CIB 119338	Libo, Guizhou, China
Elapidae	*Bungarus wanghaotingi*	CIB 119345	Mengla, Yunnan, China

OsO_4 with PBS 0.1 M, pH 7.4 for 2 h at room temperature and kept from light, and then dehydrated in ethanol and embedded in resin (EMBed 812). The resin block was cut to 60–80 nm ultrathin sections on the ultramicrotome, 2% uranium acetate saturated alcohol solution avoid light and 2.6% Lead citrate avoid CO_2 staining. The ultrathin sections are observed and recorded under TEM (Transmission Electron Microscope).

2.4. Photomicrograph acquisition Photomicrographs were obtained with a Cnoptec B302 microscope and this microscope equipped with a digital camera (Sony ICX285AQ CCD) and with Image acquisition software the ImageView in computer.

3. Results

3.1. Feeding behavior and presence of infralabial glands In this work, we observed the predatory processes and relevant behaviors of *P. berdmorei* through feeding experiments, demonstrating similar results to previous studies (Danaisawadi *et al.*, 2016; Götz, 2002), i.e., pre-capture, feeding, and post-feeding stages (Figure 1). Based on comparative anatomy, our results showed that, compared with other snake species with different feeding habits, members of the genus *Pareas* had hypertrophied infralabial glands in the lower jaw (Figure 2).

The infralabial gland in *P. berdmorei* was whitish, extended, and hypertrophied. The gland was attached to the mandible, from the anterior tip of the dentary to the anterior portion of the compound bones, and the entire gland was wrapped and dispersed in muscle (Figure 3).

3.2. General morphology of infralabial gland We investigated the glandular structure, cell types, and physiological and biochemical properties of cell contents in *P. berdmorei* and *P. chinensis* using histological and histochemical methods. Results showed that the infralabial glands were wrapped in a thin layer of connective tissue, which divided the glandular body into acinar lobules of varying size in a mesh formation (Figures 4A, 5A). The acini were typically arranged with multiple polygonal cells, predominantly mucous and seromucous cells, with large ducts formed in the middle of the mucous cells (Figures 4A, 5A). The acini contained multiple ducts formed by long columnar mucous cells surrounded by seromucous cells, which were confined to the peripheral area of the mucous cells (Figures 4A, 5A).

In *P. berdmorei*, the long columnar mucous cells usually formed ducts with mucinous properties in the central region of the acini, which were characterized by cytoplasmic secretory granules and flat basal nuclei pressed to the edge of the cell by cellular content (Figure 4C, 4D). The seromucous cells were irregular polygonal cells with round basal nuclei and cytoplasm full of secretory granules (Figure 4B, 4D). Two different types of secretory granules were observed in the seromucous cells (sm_1 and sm_2). Seromucous cell type 2 (sm_2) showed stronger reaction to periodic acid-Schiff (PAS) than seromucous cell of type 1 (sm_1). The former was less abundant, while the latter was more abundant (Figure 4E, 4F).

In *P. chinensis*, the glandular body was mainly composed of mucous and seromucous cells, with different-sized lumina. The seromucous cells were more dominant than the mucous

Figure 1 Process and behavior displays of *P. berdmorei* in predation on a snail. A: When the snail fully stretches its soft body, the snake begins to approach the snail, tilting its head and pursues the snail. B: After determining the appropriate attack position, the snake attacks and bites the snail. C: At the moment of strike, the snake inserts its mandibles into the aperture (pink arrowhead) and to lean the upper jaws against the ventral outer surface of the aperture (black arrowhead). D: After extracting the soft part of the snail, extracts the mandible from the shell, remaining snail shell and viscous mucus (black arrowhead).

cells in the acini (Figure 5B–E). Columnar mucous cells formed different-sized lumina, with flat basal nuclei and cytoplasm full of secretory granules (Figure 5C, 5D). We observed two different types of mucous cells (i.e., m_1 and m_2) based on the staining properties of their secretory granules: i.e., cells with medium granules (m_1) and cells with strong-stained granules (m_2), indicating different mucosubstances (Figure 5D). The seromucous cells formed different-sized vesicles (v), with round basal nuclei and cytoplasm containing secretory granules. We also observed two different types of seromucous cells, i.e., the more abundant type 1 (sm_1) and less abundant type 2 (sm_2), similar to *P. berdmorei* (Figure 5E, 5F).

3.3. Histochemistry of infralabial gland In *P. berdmorei*, most secretory cells of the acini were positive to both periodic acid-Schiff (PAS) and Coomassie brilliant blue R250, and negative to Alcian blue pH 2.5, indicating the seromucous nature of these cells (Figure 4B–E). The seromucous cells showed stronger positive reaction to PAS than the mucous cells, and the secretory granules in the sm_2 cells showed a stronger positive reaction to periodic acid-Schiff (PAS) than the sm_1 cells, indicating differences in protein content (Figure 4E, 4F). Duct and columnar mucous cells around the duct were strongly positive to Alcian blue pH 2.5 and negative to Coomassie brilliant blue R250, indicating their mucinous properties (Figure 4B, 4D).

In *P. chinensis*, most secretory cells were positive to both periodic acid-Schiff (PAS) and Coomassie brilliant blue R250, and negative to Alcian blue pH 2.5, similar to that observed in *P. berdmorei* (Figure 5B–E). The m_2 cells showed stronger positive reaction to Alcian blue pH 2.5 than the m_1 cells, indicating differences in mucosubstance content (Figure 5D).

3.4. Ultrastructure of infralabial gland The ultrastructure can reflect the subcellular components of secretory cells. Ultrastructural criteria are mainly based on the electron density of secretory granules, with high electron density indicating rich protein content (related to serous glands) and low electron density indicating poor protein and rich mucous content (related to mucous cells) (Kardong and Luchtel, 1986; Yoshie *et al.*, 1982). The ultrastructure of the infralabial gland in *P. berdmorei* showed that the acini were predominantly composed of secretory granules with different electron densities and polygonal cells of different sizes. A large duct was formed in the middle of the secretory cells, and lumen-facing microvilli protuberances were found near the bottom of the secretory cells (Figure 6A). These microvilli protuberances may participate in exuding secretions to the outside of the cell. The electron density of the seromucous cells was higher than that of the mucous cells. The seromucous cells contained unique spherical or elliptical granules, which were more electron-dense and
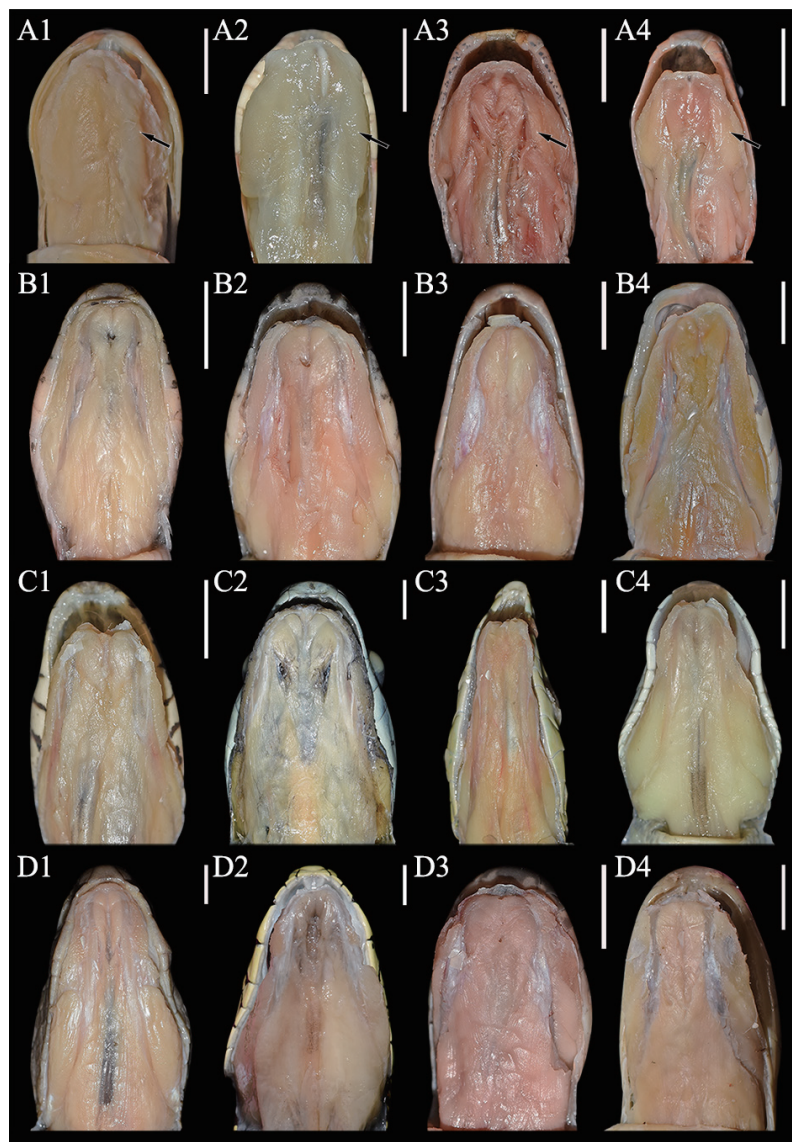
Figure 2 The lower jaw anatomy of the genus *Pareas* snakes and other snakes with different dietary habits. (A1–A4) The first row is *P. berdmorei* (CIB 119346), *P. chinensis* (CIB 119351), *P. formosensis* (CIB 119336), *P. nigriceps* (CIB 119350), respectively; (B1–B4) the second row is *Lycodon rufozonatus* (CIB 119349), *Boiga multomaculata* (CIB 119344), *Oreocryptophis porphyraceus* (CIB 119342), *Pseudoxenodon macrop* (CIB 119337), respectively; (C1–C4) the third row is *Boiga multomacula* (CIB 119347), *Boiga cyanea* (CIB 119340), *Ahaetulla prasina* (CIB 119339), *Trimeresurus guoi* (CIB 119348), respectively; (D1–D4) the fourth row is *Protobothrops mucrosquamatus* (CIB 119341), *Protobothrops jerdonii* (CIB 119343), *Bungarus multicinctus* (CIB 119338), *Bungarus wanghaotingi* (CIB 119345), respectively. The first raw is the species of *Pareas*, we observed hypertrophic infralabial glands in the lower jaw (black arrowhead), whereas other snakes with different dietary habits have not hypertrophic infralabial glands in the lower jaw. Scale bar = 5 mm.

heterogeneous when compared to mucous cells, indicating differences in cell content between the cell types (Figure 6C). Mucous cells around the duct contained uniform secretory granules with medium electron density (Figure 6B), whereas the seromucous cells contained secretory granules of varying size with higher electron density. Cytoplasm of the perinuclear region of the seromucous cells was rich in mitochondria (mi) and rough endoplasmic reticulum (er), typical characteristics of

protein-secreting cells. Desmosomes were found at the junction of adjacent cells (Figure 6D).

4. Discussion

Convergent evolution usually refers to the evolution of the same or similar phenotypes from independent lineages under similar selective pressure (Christin *et al.*, 2010; Peng *et al.*, 2022;
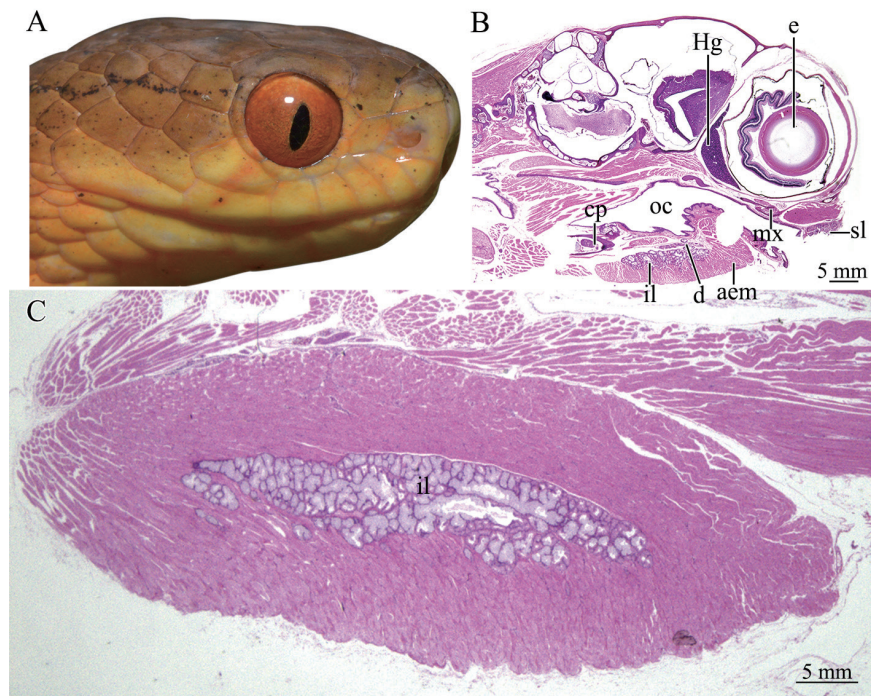
Figure 3 Histological sections of the head of *P. berdmorei*. A: Lateral view of the head of *P. berdmorei* show the hypertrophy of the lower jaw. Not to scale. B: Sagittal section of the head stained with HE, showing that the infralabial gland is attached to mandible, from the anterior tip of the dentary to the anterior portion of the compound bones, occupying approximately 80% of the total head length, the entire gland wrapped by and dispersed in associated muscle. C: Longitudinal section of the mandible, showing the entire infralabial gland wrapped by the muscle *adductor mandibulae externus medialis* (aem). Hg: harderian gland; oc: oral cavity; e: eye; mx: maxillary; sl: supralabial gland; cp: compound bone; d: dentary bone; il: infralabial gland; aem: the muscle *adductor mandibulae externus medialis*. Scale bar = 5 mm.

Stern, 2013; Storz, 2016). In Serpentes, the South American dipsadid snakes (Dipsadidae) and Asian pareid snakes (Pareidae) have evolved independently to feed exclusively on terrestrial mollusks (snails and slugs) (Götz, 2002; Sazima, 1989; Zaher *et al.*, 2019). The Pareidae family is one of the basal groups of Colubroidea, which split with other Colubroidea snakes in ~62.5 million years ago (Ma), whereas Dipsadidae is a recently evolved family, which diverged ~32.4 Ma (Li *et al.*, 2020). Previous studies have indicated that snakes in Dipsadidae developed hypertrophied infralabial glands as an adaptation to their specialized feeding behaviors (de Oliveira *et al.*, 2014; de Oliveira *et al.*, 2008; Taub, 1966). Based on comparative anatomy, our results confirmed that hypertrophic infralabial glands similar to those found in dipsadid snakes also exist in *Pareas*, suggesting that these two groups evolved convergent phenotypes to target their specialized diets.

In Dipsadidae snakes that feed exclusively on mollusks, e.g., *Dipsas* and *Sibynomorphus*, the infralabial glands are primarily composed of mucous and seromucous cells (Dunn, 1951; Kochva, 1978; Taub, 1966). In contrast, in the dipsadid genus *Atractus*, which feeds predominantly on earthworms, the infralabial glands are primarily composed of mucous cells (de Oliveira *et al.*, 2008). These results suggest that different dietary behaviors in these predators may cause differences in the composition of the infralabial glands. In our study, the two species of *Pareas* showed an infralabial gland composition similar to that of dipsadid snakes (de Oliveira *et al.*, 2008), suggesting that the seromucous cells in the infralabial glands may be specialized to snakes that feed exclusively on terrestrial mollusks. In addition, based on ultrastructural analysis, the seromucous cells were rich in cell structures correlated with protein secretion, indicating that such cells may secrete abundant proteases to aid in the digestion of food (Ichikawa and Ichikawa, 1975; Yoshie *et al.*, 1982). This is consistent with previous research reporting high protein content in infralabial gland extracts of the neotropical slug-eating snake *S. mikani* (Salomão and Laporta-Ferreira, 1994). Therefore, we speculate that seromucous cells are unique in the infralabial glands of snakes that feed on terrestrial mollusks in both Dipsadidae and Pareidae, and these cells may be responsible for digesting mollusks.

Previous studies have suggested that the secretions produced by the glands are discharged to the outside through ducts (de
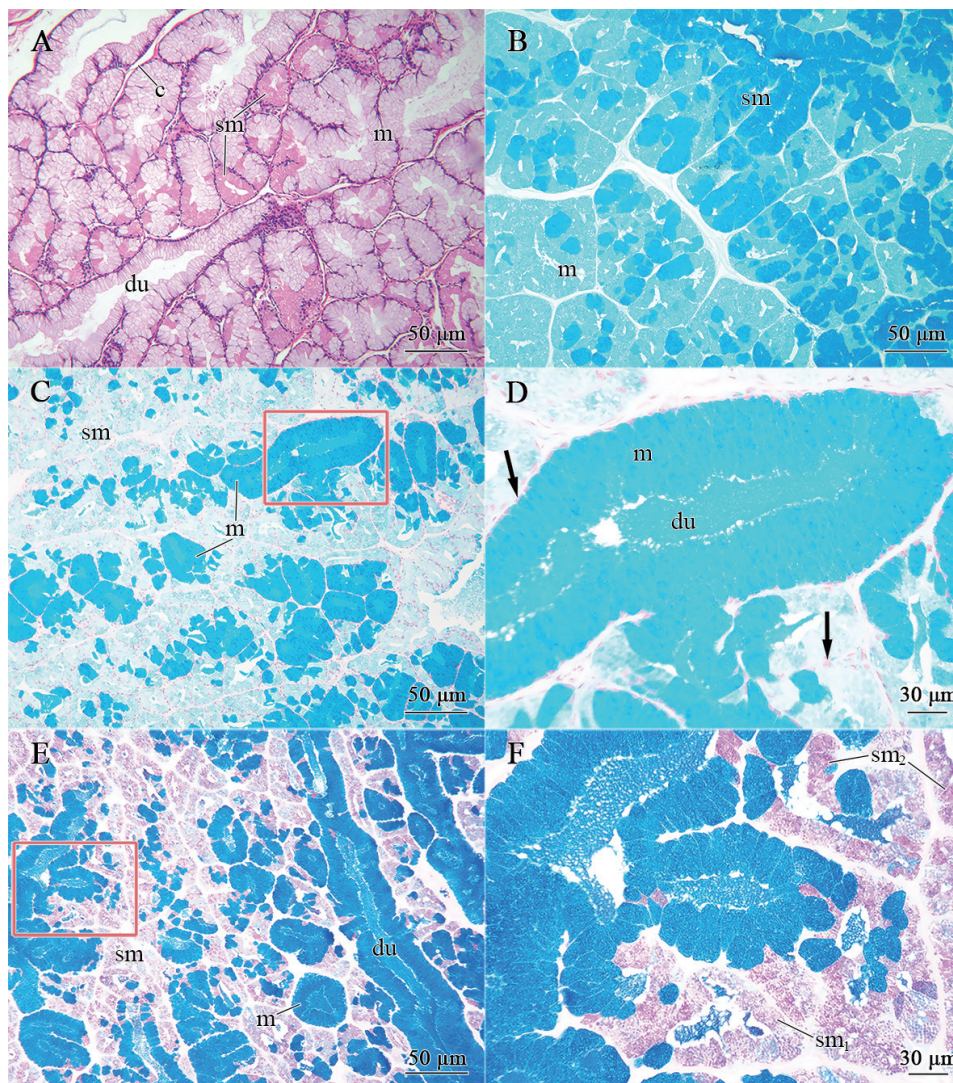
Figure 4 Morphological and histochemical condition of the infralabial glands in *P. berdmorei*. A: Sagittal section stained by Hematoxylin-eosin, showing general structure of the glandular body, mainly constituted of the duct (du) with mucous cells (m) and acini with seromucous cells (sm), divided by connective tissue (c) into acinar lobules of varying sizes. B: Transverse section stained by Coomassie brilliant blue R250 histochemical method, two types of cells have different reaction intensity, showing a strong positive reaction in seromucous cells (sm) whereas a weak positive reaction in mucous cells (m), indicating the difference in protein content between seromucous cells and mucous cells. C: Method of alcian blue, pH 2.5, showing a positive result for the mucous cells (m), indicating the presence of acid mucous, and contrasting with the seromucous cells (sm), negative to the method. Scale bar = 50 μm. D: Higher magnification of the region marked in C, stained by alcian blue, pH 2.5, showing long columnar mucous cells and flat basal nuclei (arrowhead) and ducts (du) formed in the middle. Scale bar = 30 μm. E: Longitudinal section conjugated reaction to the methods alcian blue, pH 2.5 and periodic acid-Schiff (PAS), showing mucous cells and duct have positive reaction for alcian blue, pH 2.5, while seromucous cells have lightly positive reaction for PAS. Scale bar = 50 μm. F: Higher magnification of E, showing the differences in reaction intensity of seromucous cells. The most reactive cells seem to be the seromucous type 2 (sm_2) whereas response strength of seromucous type 1 (sm_1) is relatively weak. Scale bar = 30 μm.

Oliveira *et al.*, 2016). Ducts inside glands and ducts leading to the oral cavity have been observed in neotropical goo-eating snakes (de Oliveira *et al.*, 2014; Laporta-Ferreira and Salomão, 1991). The former are receptacles for secretions generated by secretory cells, with the latter transporting these secretions to mediate physiological functions of the organism (Rosenberg, 1967). In our work, the mucous cells of the two *Pareas* species were only found in the ducts inside the glands, thus showing a similar distribution pattern as found in some dipsadid snakes (de Oliveira *et al.*, 2014; de Oliveira *et al.*, 2008). This pattern
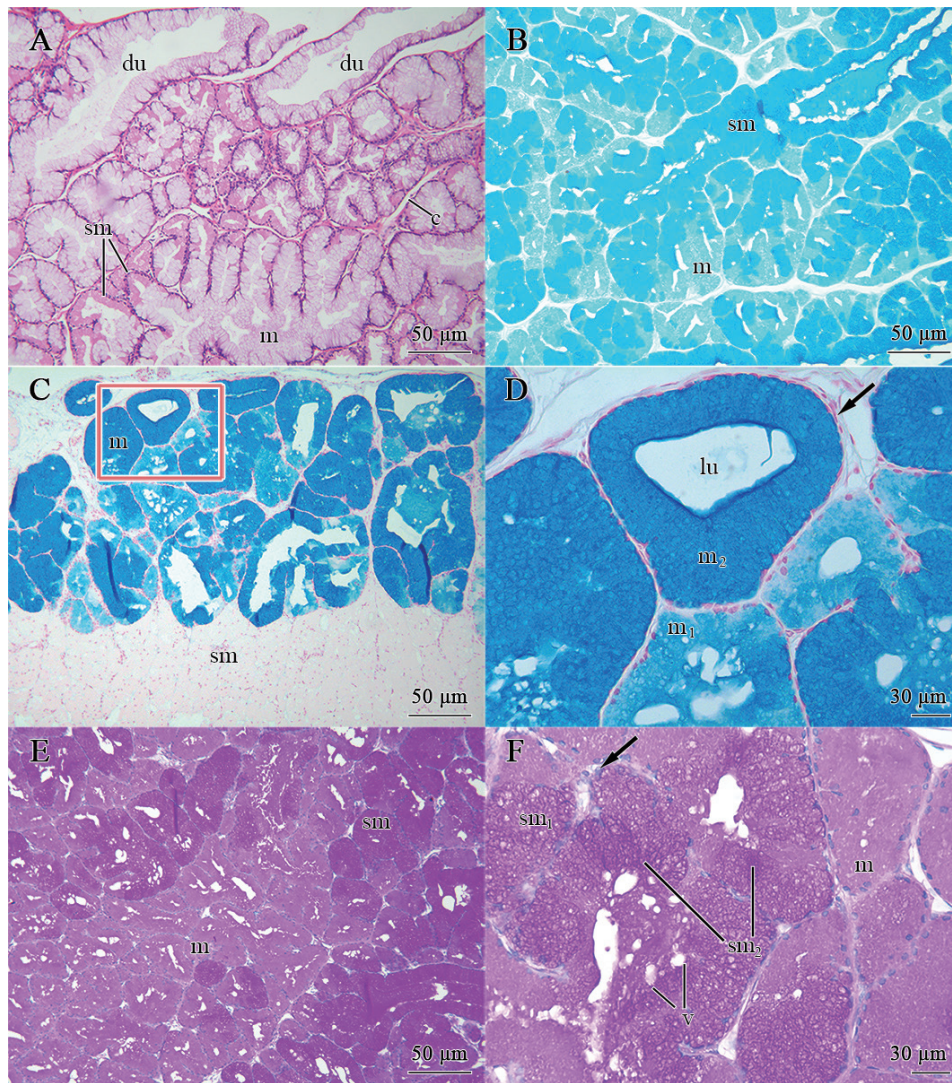
Figure 5 Morphological and histochemical condition of the infralabial glands in *P. chinensis*. A: General structure of the glandular body, mainly constituted of the duct (du) with mucous cells (m) and acini with seromucous cells (sm), divided by connective tissue (c) into lobules of varying sizes. B: Sagittal section stained by Coomassie brilliant blue R250 histochemical method, showing a strong positive reaction in seromucous cells (sm) whereas a weak positive reaction in mucous cells (m). C: Alcian blue, pH 2.5 histochemical method, showing positive results for two types of mucous cells (m) and a negative result for the seromucous cells (sm), indicating a different type of mucous content in these cells. Scale bar = 50 μm. D: Higher magnification of glandular body marked in C, showing a few large acini, which are constituted of mucous cells (m), with flat basal nuclei (arrowhead), two types of mucous cells (m), i.e., m_2 have more strongly positive reaction to alcian blue, pH 2.5 than m_1. Scale bar = 30 μm. E: Sagittal section stained by method of periodic acid-Schiff (PAS), showing all types of cells are positive result to PAS, only varying in intensity, in each type. Scale bar = 50 μm. F: Higher magnification of E, showing the differences in reaction intensity of each cell type. The seromucous cells have stronger reaction to PAS than mucous cells, and have round basal nuclei (arrowhead). The seromucous type 2 (sm_2) have stronger positive reaction whereas seromucous type1 (sm_1) has a weaker reaction intensity. Some vesicles (v) of varying sizes filled with secretory granules among these cells. Scale bar = 30 μm.

facilitates the transportation and release of secretions generated by glandular cells (Taub, 1967; 1966; Yoshie *et al.*, 1982). However, we did not observe ducts leading the oral cavity, possibly due to wrong anatomical methods and sectional angles. Therefore, how seromucous cell secretions are transported through the surrounding ducts in *Pareas* needs to be further researched.
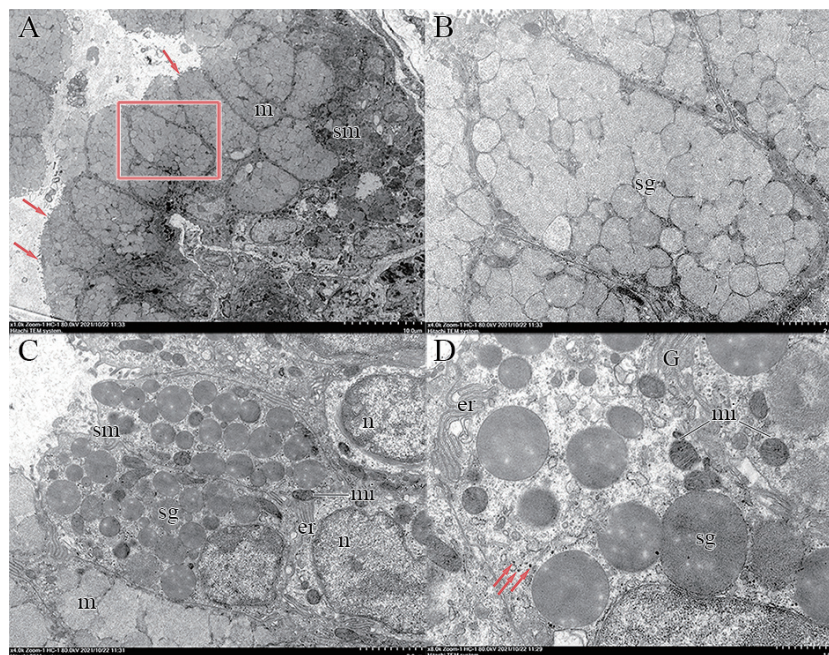
Figure 6 Transmission electron microscopy of the infralabial gland of *P. berdmorei*. A: Sagittal section of the gland show that acinus is composed of most polygonal cells, packed with medium electron dense homogeneous secretory granules in mucous cells (m) and other type of cell present on the periphery of mucous cells, cytoplasm packed with elliptical high electron dense secretory granules in seromucous cells (sm), and in the apical membrane of all types of secretory cells have microvilli facing the lumen. m: mucous cells; sm: seromucous cells; arrowhead: microvilli. Scale bar = 10 μm. B: Higher magnification of mucous cells and cytoplasm packed with medium-electrodense granules (sg). C: Detail of cytoplasm of the seromucous cells (sm), show difference of electron density secretory granules between mucous and seromucous cells, among them, the seromucous cells contain high electron density granules of varying sizes and irregular basal nucleus (n), rich in endoplasmic reticulum and mitochondria. n: nuclei; mi: mitochondria; er: endoplasmic reticulum; sg: secretory granules. Scale bar = 2 μm. D: Higher magnification of seromucous cells shows that have abundant mitochondria, rough endoplasmic reticulum and Golgi apparatus. There are round or oval desmosomes between adjacent cells. G: Golgi apparatus; arrowhead: desmosomes. Scale bar = 1 μm.

References

Broadley D. G. 1979. Predation on reptile eggs by African snakes of the genus *Prosymna*. Herpetologica, 35(4): 338–341

Chang K. X., Huang B. H., Luo M. X., Huang C. W., Wu S. P., Nguyen H. N., Lin S. M. 2021. Niche partitioning among three snail-eating snakes revealed by dentition asymmetry and prey specialisation. J Anim Ecol, 90(4): 967–977

Christin P. A., Weinreich D. M., Besnard G. 2010. Causes and evolutionary significance of genetic convergence. Trends Genet, 26(9): 400–405

Coleman K., Rothfuss L. A., Ota H., Kardong K. V. 1993. Kinematics of egg-eating by the specialized Taiwan snake *Oligodon formosanus* (Colubridae). J Herpetol, 27(3): 320–327

Cundall D., Greene H. W. 2000. Feeding in snakes. In: Schwenk, K. (Ed.), Feeding: Form, Function, and Evolution in Tetrapod Vertebrates. San Diego: Academic Press, 293–333

Danaisawadi P., Asami T., Ota H., Sutcharit C., Panha S. 2016. Predatory behavior of the snail-eating snake *Pareas carinatus* (Boie, 1828) (Squamata: Pareidae): An ethogram study. Trop Nat Hist, 16(4): 21–31

de Oliveira L., da Costa Prudente A. L., Zaher H. 2014. Unusual labial glands in snakes of the genus *Geophis* Wagler, 1830 (Serpentes: Dipsadinae). J Morphol, 275(1): 87–99

de Oliveira L., Jared C., da Costa Prudente A. L., Zaher H., Antoniazzi M. M. 2008. Oral glands in dipsadine "goo-eater" snakes: Morphology and histochemistry of the infralabial glands in *Atractus reticulatus*, *Dipsas indica*, and *Sibynomorphus mikanii*. Toxicon, 51(5): 898–913

de Oliveira L., Scartozzoni R. R., de Almeida-Santos S. M., Jared C., Antoniazzi M. M., Salomão M. D. G. 2016. Morphology of Duvernoy's glands and maxillary teeth and a possible function of the Duvernoy's gland secretion in *Helicops modestus* Gunther, 1861 (Serpentes: Xenodontinae). S Am J Herpetol, 11(1): 54–65

Deepak V., Ruane S., Gower D. J. 2018. A new subfamily of fossorial

colubroid snakes from the Western Ghats of peninsular India. J Nat Hist, 52(45): 2919–2934

dos Santos M. M., da Silva F. M., Hingst-Zaher E., Machado F. A., Zaher H., Prudente A. L. 2017. Cranial adaptations for feeding on snails in species of *Sibynomorphus* (Dipsadidae: Dipsadinae). Zoology, 120: 24–30

Dunn E. R. 1951. The status of the snake genera *Dipsas* and *Sibon*, a problem for "quantum evolution.". Evolution, 5(4): 355–358

Götz M. 2002. The feeding behavior of the snail-eating snake *Pareas carinatus* Wagler 1830 (Squamata : Colubridae). Amphibia-Reptilia, 23(4): 487–493

Greene H. W. 1997. Snakes: the evolution of mystery in nature. Berkeley: University of California Press, 1–357

Hoso M. 2017. Asymmetry of mandibular dentition is associated with dietary specialization in snail-eating snakes. PeerJ, 5: e3011

Hoso M., Asami T., Hori M. 2007. Right-handed snakes: convergent evolution of asymmetry for functional specialization. Biol Lett, 3(2): 169–173

Ichikawa M., Ichikawa A. 1975. The fine structure of the parotid gland of the *Mongolian gerbil, Meriones meridianus*. Arch Hist Japon, 38(1): 1–16

Jayne B. C., Voris H. K., Ng P. K. 2018. How big is too big? Using crustacean-eating snakes (Homalopsidae) to test how anatomy and behaviour affect prey size and feeding performance. Biol J Linn Soc, 123(3): 636–650

Kardong K. V., Luchtel D. L. 1986. Ultrastructure of Duvernoy's gland from the wandering garter snake, *Thamnophis elegans vagrans* (Serpentes, Colubridae). J Morphol, 188(1): 1–13

Kiernan J. 2015. Histological and Histochemical Methods: Theory and Practice. 5th ed. London: Scion Publishing Press, 1–588

Kochva E. 1978. Oral glands of the reptilia. In: Gans C, editor. Biology of the Reptilia, Vol. 8. New York: Academic Press, 1–782

Kojima Y., Fukuyama I, Kurita T., Bin Hossman M. Y., Nishikawa K. 2020. Mandibular sawing in a snail-eating snake. Sci Rep, 10(1): 1–5

Laporta-Ferreira I. L., Salomão M. D. G. 1991. Morphology, physiology and toxicology of the oral glands of a tropical cochleophagous snake, *Sibynomorphus neuwiedi* (Colubridae-Dipsadinae). Zool Anz, 227(3): 198–208

Li J. N., Liang D., Wang Y. Y., Guo P., Huang S., Zhang P. 2020. A large-scale systematic framework of Chinese snakes based on a unified multilocus marker system. Mol Phylogen Evol, 148: 106807

Lillywhite H. B. 2014. How Snakes Work: Structure, Function and Behavior of the World's Snakes. New York: Oxford University Press, 37–75

Peng Z. L., Wu W., Tang C. Y., Ren J. L., Jiang D., Li J. T. 2022. Transcriptome analysis reveals olfactory system expression characteristics of aquatic snakes. Front Genet, 13: 825974

Peters J. A. 1960. The snakes of the subfamily Dipsadinae. Miscellaneous Publications, Museum of Zoology, University of Michigan, 114: 1–224

Poyarkov N. A., Nguyen T. V., Pawangkhanant P., Yushchenko P. V., Brakels P., Nguyen L. H., Nguyen H. N., Suwannapoom C., Orlov N., Vogel G. 2022. An integrative taxonomic revision of slug-eating snakes (Squamata: Pareidae: Pareineae) reveals unprecedented diversity in Indochina. PeerJ, 10: 1–99

Rosenberg H. I. 1967. Histology, histochemistry, and emptying mechanism of the venom glands of some elapid snakes. J Morphol, 123(2): 133–155

Sabatini D. D., Bensch K., Barrnett R. J. 1963. Cytochemistry and electron microscopy. The preservation of cellular ultrastructure and enzymatic activity by aldehyde fixation. J Cell Biol, 17(1): 19–58

Salomão M. D. G., Laporta-Ferreira I. L. 1994. The role of secretions from the supralabial, infralabial, and Duvernoy's glands of the slug-eating snake *Sibynomorphus mikanii* (Colubridae: Dipsadinae) in the immobilization of molluscan prey. J Herpetol, 28(3): 369–371

Sazima I. 1989. Feeding behavior of the snail-eating snake, *Dipsas indica*. J Herpetol, 23(4): 464–468

Stern D. L. 2013. The genetic causes of convergent evolution. Nat Rev Genet, 14(11): 751–764

Storz J. F. 2016. Causes of molecular convergence and parallelism in protein evolution. Nat Rev Genet, 17(4): 239–250

Taub A. M. 1966. Ophidian cephalic glands. J Morphol, 118(4): 529–541

Taub A. M. 1967. Comparative histological studies on Duvernoy's gland of colubrid snakes. Bull Am Mus Nat Hist N Y, 138: 1–50

Wang P., Che J., Liu Q., Li K., Jin J. Q., Jiang K., Shi L., Guo P. 2020. A revised taxonomy of Asian snail-eating snakes *Pareas* (Squamata, Pareidae): evidence from morphological comparison and molecular phylogeny. Zookeys, 939: 45–64

Webb J. K., Shine R., Branch W. R., Harlow P. S. 2000. Life-history strategies in basal snakes: reproduction and dietary habits of the African thread snake *Leptotyphlops scutifrons* (Serpentes: Leptotyphlopidae). J Zool, 250(3): 321–327

Yoshie S., Ishiyama M., Ogawa T. 1982. Fine structure of Duvernoy's gland of the japanese colubrid snake, *Rhabdophis tigrinus*. Arch Hist Japon, 45(4): 375–384

Zaher H., de Oliveira L., Grazziotin F. G., Campagner M., Jared C., Antoniazzi M. M., Prudente A. L. 2014. Consuming viscous prey: a novel protein-secreting delivery system in neotropical snail-eating snakes. BMC Evol Biol, 14(1): 1–28

Zaher H., Murphy R. W., Arredondo J. C., Graboski R., Machado-Filho P. R., Mahlow K., Montingelli G. G., Quadros A. B., Orlov N. L., Wilkinson M., Zhang Y. P., Grazziotin F. G. 2019. Large-scale molecular phylogeny, morphology, divergence-time estimation, and the fossil record of advanced caenophidian snakes (Squamata: Serpentes). PLoS ONE, 14(5): e0216148

Zhao E. M. 2006. Snakes of China. Vol. 1. Hefei: Anhui Science Technology Publishing House, 243–245 (in Chinese)

Zug G. R. 1993. Herpetology: An Introductory Biology of Amphibians and Reptiles. San Diego: Academic Press, 1–527

Handling Editor: Heling Zhao